physiologia

MDPI

Article

Investigating the Effectiveness of Plant-Mediated Cerium Oxide Nanoparticles as Larvicidal Agents against the Dengue Vector *Aedes aegypti*

Pratik P. Dhavan [1,2,*], Vivek R. Sonawane [2] and Abhinava K. Mishra [1,*]

[1] Molecular, Cellular and Developmental Biology Department, University of California Santa Barbara, Santa Barbara, CA 93106, USA
[2] Department of Life Sciences, University of Mumbai, Vidyanagari Campus, Santacruz (East), Mumbai 400098, India
* Correspondence: pratikdhavan@ucsb.edu (P.P.D.); abhinavamishra@ucsb.edu (A.K.M.)

Abstract: *Aedes aegypti* mosquito is responsible for the transmission of some of the most serious vector-borne diseases affecting humans, including dengue fever, chikungunya, and Zika. The only effective method for minimizing their transmission is vector control. In this work, an environmentally friendly method for synthesizing cerium oxide nanoparticles (CeO_2 NPs) is highlighted, and the larvicidal activity against *Ae. aegypti* was studied. This method uses the aqueous extract of *Bruguiera cylindrica* leaves (BL) as an oxidizer and stabilizing agent. UV–Vis spectroscopy presented a distinctive absorbance band at 303 nm for CeO_2 NPs with a band gap of 3.17 eV. The functional groups from the plant extract connected to CeO_2 NPs were identified by FT-IR analysis, while X-ray diffraction revealed the cubic fluorite orientation of CeO_2 NPs. Zeta potential revealed a surface charge of −20.7 mV on NPs. The formation of CeO_2 NPs was confirmed by an energy dispersive spectral analysis, and TEM and DLS revealed an average diameter of 40–60 nm. The LC_{50} of synthesized CeO_2 against *Ae. aegypti* fourth instar larvae was reported to be 46.28 µg/mL in 24 h. Acetylcholinesterase (47%) and glutathione S-transferase (13.51%) activity were significantly decreased in *Ae. aegypti* larvae exposed to synthesized CeO_2 NPs versus the control larvae. All these findings propose the potential for using *B. cylindrica* leaves-synthesized CeO_2 NPs as an efficient substitute for insecticides in the management of mosquitoes.

Keywords: green synthesis; cerium oxide nanoparticles; *Bruguiera cylindrica* extract; larvicidal activity; acetylcholinesterase activity; glutathione S-transferase activity

Citation: Dhavan, P.P.; Sonawane, V.R.; Mishra, A.K. Investigating the Effectiveness of Plant-Mediated Cerium Oxide Nanoparticles as Larvicidal Agents against the Dengue Vector *Aedes aegypti*. *Physiologia* **2023**, *3*, 329–346. https://doi.org/10.3390/physiologia3020023

Academic Editor: M. Leonor Cancela

Received: 13 December 2022
Revised: 12 April 2023
Accepted: 4 May 2023
Published: 12 May 2023

1. Introduction

The insect-borne disease is still a major cause of illness and death around the world. Mosquitoes alone infect more than 700 million people each year [1]. Mosquitoes are responsible for dreadful diseases such as malaria, filariasis, dengue hemorrhagic fever, and others that are prevalent worldwide [2–4].

Due to the challenges in controlling both the disease and its carrier mosquitoes, dengue is a fatal mosquito-borne disease that has gained worldwide attention [5,6]. Female *Ae. aegypti* and *Ae. albopictus* mosquitos are the primary vectors of this disease. Dengue virus serotypes (DEN-1, DEN-2, DEN-3, and DEN-4) have been identified as distinct but closely related [7]. Dengue fever's global prevalence has increased dramatically in recent decades. An estimated 390 million infections occur each year, putting half of the world's population at risk [8]. Furthermore, *Ae. aegypti* and *Ae. albopictus* mosquitoes transmit yellow fever, chikungunya, and the recently identified Zika virus (ZIKV), for which there is currently no vaccine, and dengue fever, for which the vaccine is still being evaluated in the field [6,9]. Therefore, mosquito control is the best way to reduce the transmission of mosquito-borne diseases to humans. Mosquito control programs may employ methods

such as removing mosquito larval habitats, applying larvicides to kill mosquito larvae, or spraying insecticides from trucks or aircraft to kill adult mosquitoes [10].

Synthetic insecticides commonly used in mosquito control programs have negative effects on the environment, human health, and non-target organisms, and have resulted in insecticide-resistant mosquitoes. With the increased use of synthetic insecticides, there has been evidence of mosquito resistance to organophosphates as a result of consistent spraying and application. Metabolic enzymes such as acetylcholinesterase (AChE) and glutathione S-transferase (GST) are important in determining whether or not mosquito larvae are susceptible to these insecticides [11]. Mosquito vectors with AChE genes have developed a resistance to synthetic insecticides, particularly temephos. Chemical pesticides target the AChE enzyme, which degrades acetylcholine, a neurotransmitter that transmits nerve impulses across synaptic gaps [12]. Insects also express GST, a detoxifying enzyme that aids in the neutralization of xenobiotic toxicity [13]. Thus, metabolic enzymes are an important tool for determining mosquito larvae and adult susceptibility to insecticides.

In response to selection pressures from herbivores and microbes, many marine plants synthesize a variety of chemically varied secondary metabolites, some of which act as insecticides. Many natural plant compounds have ovicidal, pupicidal, adult-repellent, growth, and/or breeding inhibitor properties [14]. *B. cylindrica* is a Rhizophoraceae family of evergreen mangrove found throughout Asia, including the Pacific region, Southeast Asia, and western India [15]. *B. cylindrica* contains a variety of phytochemicals, including fatty acids, flavonoids, tannins, terpenes, alkaloids, and glycosides [16]. As a result, in folk medicine, *B. cylindrica* has been used to treat diarrhea and wound healing. Different parts of *B. cylindrica* is also used to treat hemorrhage, and ulcers [17], acting as antimicrobial [18–20], antioxidant [21], and as antiviral [22]. The ability of nanoparticles derived from this mangrove plant to kill mosquito larvae is another area that has recently been investigated [23].

Green technologies have lately been demonstrated to be a viable technique for minimizing the use of chemical pesticides, as misuse of these products is frequently associated with enormous non-target effects and widespread resistance [24]. Because of their high surface-to-volume ratio, nanoparticles have a variety of physical and chemical characteristics. The physiochemical features of nanoscale NPs, as well as their ability to modify numerous cellular and organismal responses have been harnessed for medicinal applications such as immunotherapy, medication transport, and vaccine production [25]. Cerium oxide (CeO_2) is a material with a broad band energy (3.19 eV) and high exciton-binding energy [26]. It is used in a number of industries, including electronics [27], biosensors [28], drug delivery [29], agronomy [30], health sciences [31], etc. Many physical, chemical, and biological (plants and microorganisms) approaches are used to create CeO_2 nanoparticles (CeO_2 NPs) [32,33]. Plant-based methods provide safer routes for preparing CeO_2 NPs, and they are potentially useful for pharmaceutical applications [34]. Moreover, plant extract phytochemicals such as polysaccharides, flavonoids, phenolic acids, and alkaloids have been shown to effectively reduce metal ions. Furthermore, phytochemicals play an important role in the capping, stabilization, and chelation of NPs during their formation. As a result, phytochemicals are ideal entities for nanoparticle biosynthesis. The biosynthesis of nanoparticles with plants also improves the safety profile of nanoparticles by lowering the expected toxicity [35–37]. Thus, in the present study, *B. cylindrica* leaves were used to synthesize CeO_2 nanoparticles, and their larvicidal properties were tested on the dengue vector *Ae. aegypti.*

2. Materials and Methods

The water used throughout the experiments was purified using Millipore Milli-Q (18.2 MΩ.cm at 25 °C) purification system. Cerium(III) nitrate hexahydrate salt ($Ce(NO_3)_3 \cdot 6H_2O$) (catalogue no. 102271), reduced glutathione (GSH) (catalogue no. 3541), 1-chloro2,4-dinitrobenzene (CDNB) (catalogue no. 102427), 5,5′-dithiobis-2-nitrobenzoic acid (DTNB)

(catalogue no. 322123) was procured from Sigma-Aldrich, India. Acetylthiocholine iodide (ACT) (catalogue no. RM770) were purchased from Hi-Media (Mumbai, India).

2.1. Preparation of B. cylindrica Plant Extract

The *B. cylindrica* leaves were collected from the Bhatye beach region in the Ratnagiri District of Maharashtra, India, and verified by a professional taxonomist. The coordinates for this area are 16°58′44.0691″ N and 73°17′38.7499″ E. *B. cylindrica* leaves were washed, oven-dried at 40 °C for a week to reduce fungal contamination, and ground into a powder. To make the aqueous BL extract, 5 g of plant powder was dispersed with 100 mL of Milli-Q water (MQ-W) and heated in a water bath at 100 °C for 20 min. With the help of No. 42 Whatman filter paper, the filtrate and residue were separated (42 ashless diameter 125 mm GE Healthcare Life Sciences).

2.2. Qualitative Phytochemical Analysis of BL Aqueous Extract

Phytochemical analysis of all the extracts were studied as follows [38,39]:

2.2.1. Alkaloids

A few drops of Meyer's reagent (potassium mercuric chloride solution) were added into 1 mL extract. A creamish-white precipitate formed, indicating the presence of alkaloids.

2.2.2. Phenolic Compounds

An amount of 0.5 mL of 1% lead acetate and 0.2 mL of 1% ferric chloride were added to the 1 mL extract. A blue-black precipitate with lead acetate and a green-brown precipitate with ferric chloride was obtained in the extract.

2.2.3. Flavonoids

An amount of 0.2 mL of plant extract was taken in a test tube and mixed with 1 mL of 10% sodium hydroxide solution. Formation of an intense yellow color was seen. To this, 0.5 mL of diluted hydrochloric acid was added. Yellow solution that later turns colorless would indicate the presence of flavonoids.

2.2.4. Saponins

An amount of 5 mL extract was agitated in a graduated cylinder for 15 min. Formation of foam indicated the presence of saponins.

2.2.5. Steroids

An amount of 1 mL extract was dissolved in 10 mL chloroform and an equal volume of concentrated sulfuric acid was added by the sides of the test tube. The upper layer turned red and the sulfuric acid layer showed yellow with green fluorescence. This indicated the presence of steroids.

2.2.6. Terpenoids

In 2 mL of extract, 2 mL of acetic anhydride and 2 mL of concentrated sulfuric acid were added. The presence of terpenoids is denoted by the formation of blue-green rings.

2.2.7. Tannins

In 0.5 mL of the extract, about 10 mL of bromine water was added. Decolorization of bromine water indicated the presence of tannins.

2.2.8. Reducing Sugars

An amount of 0.5 mL of aqueous extracts was mixed with Fehling's I and II solutions and boiled for half an hour in water bath. Formation of red precipitation indicated the presence of reducing sugars.

2.2.9. Proteins

An amount of 0.5 mL of aqueous extract was mixed with equal volumes of 5% sodium hydroxide and copper sulfate. Formation of violet color indicated the presence of proteins.

2.3. Production of Cerium Oxide Nanoparticles (CeO_2 NPs)

Cerium oxide (IV) nanoparticles (CeO_2 NPs) were synthesized using a precipitation reaction in which cerium nitrate, BL aqueous extract, and distilled water were used as the cerium precursor, stabilizing agent, and solvent, respectively. To begin the synthesis, 20 mL of 10 mM cerium nitrate dissolved in MQ-W was carefully added to 80 mL of 5% BL extract. The mixture solution was stirred at 60 °C for 6 h to obtain a lemon-colored precipitate. To complete the process, the precipitate were calcined for 2 h at 400 °C, yielding CeO_2 NPs in powdered form.

2.4. Characterization

To verify the synthesis of nanoceria, the UV–visible spectrometer Shimadzu UV–1800 (λ = 200–800 nm) was used to record the UV–Vis absorption spectrum of CeO_2 NPs after 24 h. Fourier transform infrared spectroscopy (FTIR) (Perkin Elmer Frontier, 91579) was used to detect different functional groups linked with the synthesis of CeO_2 NPs and BL aqueous extract (5% vacuum lyophilized), utilizing the KBr pelleting process. Crystalline nature of synthesized CeO_2 NPs was recorded using X-ray diffraction (XRD) at a voltage of 40 kV and a current of 40 mA, with Cu Kα radiation (1.54 Å) in a θ–2θ configuration using Bruker D8 Discover model (Bruker, Germany). Transmission electron microscopy (TEM) and energy-dispersive spectra (EDS) were used to evaluate the size and morphology of produced nanoceria (FEI, Tecnai G2 model). The zeta potential and dynamic light scattering were used to examine the surface charge and hydrodynamic size of nanoceria (Nanoseries Nano-ZS90, Malvern Instruments, Malvern, UK).

2.5. Rearing of Mosquito and Larvicidal Activity

Ae. aegypti larvae were collected from the Vidyanagari campus, University of Mumbai, India and neighboring localities. *Ae. aegypti* larvae were identified [40], and the lab's larval colony was maintained at 28 °C, relative humidity (RH) was held between 70–80%, and a 14:10 h of light and dark photoperiod [41]. Adults were given a 2% sucrose solution soaked in non-absorbent cotton. Female mosquitos were fed blood meals for egg development using the membrane feeding method [42]. The eggs were collected in a bowl lined with Whatman filter paper and allowed to hatch on sterile Petri dishes with dechlorinated water (PS, 150 × 20 mm). A 2:1 mixture of yeast powder and dog biscuits (Meatup dry food) was fed to the larvae. Pupae that had grown into adults were collected and transferred to glass cages for adult emergence.

The WHO standard method was used to investigate the larvicidal activity of BL aqueous extract and CeO_2 NPs [43]. In order to prepare a graded series of concentrations, BL extract and CeO_2 NPs were distributed in dechlorinated water (250 µg/mL to 2500 µg/mL for aqueous BL extract and 10 µg/mL to 70 µg/mL for synthetic CeO_2 NPs). Furthermore, early fourth instar *Ae. aegypti* larvae were placed in batches of 20 in 250 mL plastic cups containing 199 mL distilled water (DW) and 1 mL of each treatment in graded concentrations. The experimental treatments were carried out in triplicate, along with a control group. Only 200 mL of distilled water was used in the control group. Larval motility was determined by measuring larval movement after 24 h of treatment.

2.6. Enzymatic Studies

To investigate neurotoxicity and foreign material detoxification, the effects of BL aqueous extract and BL-produced CeO_2 NPs on AChE and GST enzymes in *Ae. aegypti* larvae were examined. Sublethal doses (LC_{50}) of BL extract and CeO_2 NPs treatment were given to early fourth instar larvae over a period of 24 h. Only the live larvae from the control, BL extract, and CeO_2 NPs treatments were selected for additional biochemical

analysis after 24 h, because it is preferable to determine the impact of a toxicant on the organism at the time of evaluation but before mortality occurs.

2.6.1. Whole-Body Homogenates for Enzyme Source Preparation

After 24 h, 10 larvae treated with BL aqueous extract, CeO_2 NPs (test) and control (untreated) were retrieved from each of the treatment groups, cleaned with double distilled water, then blotted with tissue paper to remove any adhering water. The larvae were then collected and homogenized in Eppendorf^{TM} tubes (held on ice) with a Teflon hand homogenizer in 0.5 mL of phosphate buffer (100 mM phosphate buffer (pH 7.2) and 1% Triton X-100) [44]. The homogenate was centrifuged at 10,000× *g* for 15 min at 4 °C, and the supernatant was used as the enzyme source. The enzyme protein source was calculated using the Bradford technique [45].

2.6.2. AChE Activity

Using acetylthiocholine iodide (ACT) as a substrate, AChE activity was measured spectrophotometrically in whole body homogenates of larvae using a modified method of Ellman et al. [46,47]. An aliquot of 100 µg/mL crude enzyme homogenate was combined with 450 µL of pH 7.5 sodium phosphate buffer, 50 µL of 10 mM DTNB, and 50 µL of 12.5 mM acetylthiocholine iodide. After incubating the sample at room temperature for 5 min, the optical density of the sample at 400 nm was determined in comparison to an appropriate reagent blank using a spectrophotometer (Shimadzu, UV–1800). Using a reported extinction coefficient (ε = 13.6 mM^{-1} cm^{-1}), AChE activity was represented as µmol ACT hydrolyzed/min/mg protein.

2.6.3. GST Activity

To 100 µL of larval homogenate (100 µg/mL crude enzyme), 100 µL of 30 mM CDNB was added, and the volume was adjusted to 500 µL with sodium phosphate buffer. After a 5 min preincubation at 37 °C, 100 µL of 30 mM GSH was added to the reaction mixture. Absorbance was measured at 340 nm at 1 min intervals for 5 min. We ran the experiment without the enzyme as a control. GST activity was estimated as µmol CDNB hydrolyzed/min/mg protein using the previously published extinction coefficient (ε = 9.6 mM^{-1} cm^{-1}) [48].

2.7. Statistical Data Analysis

The LC_{50} and LC_{90} values were calculated from a log dosage–probit mortality regression line using the SPSS version 21.5 software program [49]. Data were reported as mean ± SEM. To examine the difference in enzyme inhibition between the control and treatment groups, one-way variance analysis (ANOVA) was used, followed by the post hoc Tuckey test. Results with $p < 0.05$ were considered statistically significant.

3. Results

3.1. Qualitative Phytochemical Analysis of BL Aqueous Extract

Phytochemicals present in the plant extracts play an important role in larvicidal activity and the synthesis of NPs. In this study, the leaves of *B. cylindrica* were screened for the presence of major phytochemical groups. Alkaloids, flavonoids, terpenoids, tannins, saponins, proteins, phenolic compounds, and reducing sugars were discovered during the preliminary phytochemical screening (Table 1).

3.2. Characterization of CeO_2 NPs

3.2.1. UV–Visible Spectroscopy

B. cylindrica leaves extract has been used in this study as an agent for nanoceria's green synthesis. The phytochemicals in the leaves of *B. cylindrica* were active in oxidizing, capping, and stabilizing cerium ions to CeO_2 NPs. By measuring the absorption at 200–800 nm, the formation of CeO_2 NPs was monitored by UV–Vis spectroscopy.

Table 1. Qualitative phytochemical analysis of the aqueous extract of *B. cylindrica* leaves.

Phytochemical Constituents	*B. cylindrica* *Leaf aqueous* Extract
Alkaloids	+
Flavonoids	+
Terpenoids	+
Steroids	−
Tannins	+
Saponins	+
Phenolic compounds	+
Reducing sugars	+
Proteins	+

(+) indicate the presence of phytochemicals and (−) indicate the absence of phytochemicals.

Optical band gap energy (Eg) for a semiconductor can be determined by Equation (1), in which, hν is the photon energy, α is the absorption coefficient, B is a constant (relates to the material), and n is 2 or 0.5 for direct or indirect transitions, respectively. It was proven that the transition of ceria is direct [50]; therefore, the value of n is 2 here:

$$(\alpha h\vartheta)^n = B(h\vartheta - Eg) \quad (1)$$

The appearance of a peak at 303 nm in the UV–visible spectrum confirmed the formation of CeO_2 NPs (Figure 1a). Figure 1b illustrates the plot of $(\alpha h\nu)^2$ vs. hν, which was used to calculate the band gap energy of CeO_2 NPs. The band gap was found to be 3.17 eV as compared to the band gap value (3.19 eV) already reported in the literature for the CeO_2 NPs [51]. When NPs were synthesized using BL aqueous extract, they showed a slight red shift in the band gap which may be associated with oxygen vacancies and the existence of Ce^{3+} to the nanoparticle surface. Oxygen defects and Ce^{3+} ions generate intermediate defect energy states in the CeO_2 band gap. Due to the presence of these states, the direct transition of electrons from O 2p to Ce 4f is slowed down, resulting in the decrease in band gap value [50].

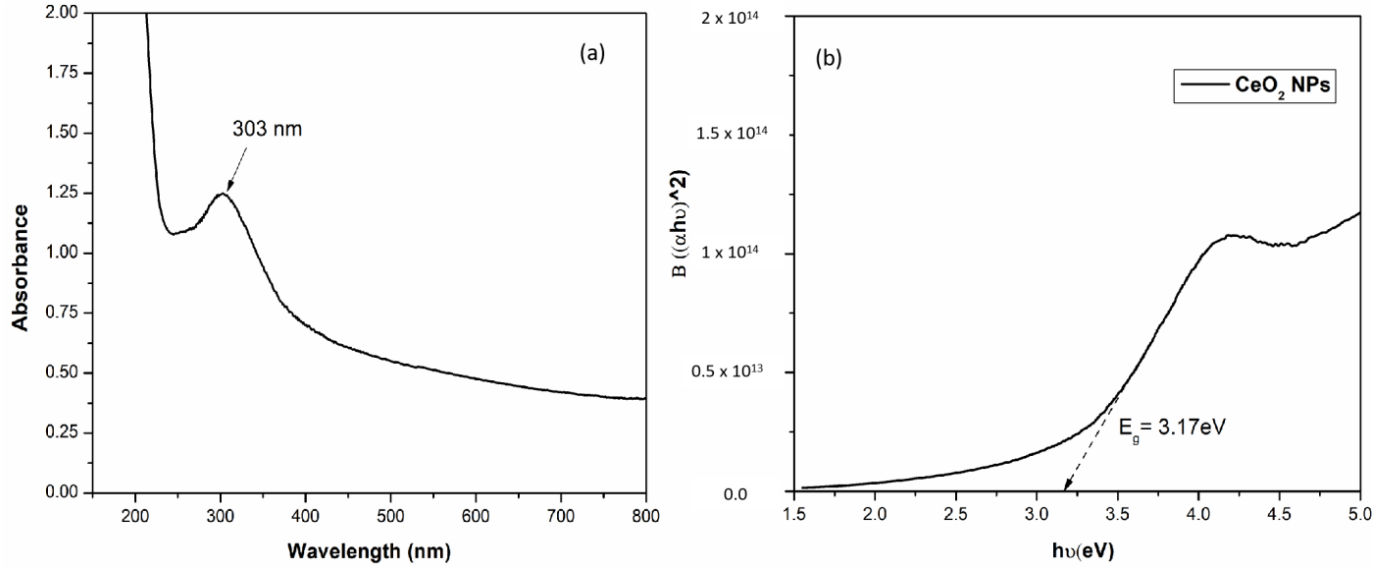

Figure 1. (**a**) UV–visible spectra of CeO_2 NPs synthesized using BL extract. (**b**) Band gap of CeO_2 NPs using Tauc plot.

3.2.2. XRD Analysis

The nanoceria's XRD pattern shown in Figure 2 confirms the crystalline nature of synthesized CeO_2 NPs. The high-intensity peaks identified at 2θ°- 28.8°, 33.4°, 47.7°, 56.6°, 59.3°, and 69.7° corresponded to the cubic fluorite crystal orientation planes (111), (200), (220), (311), (222), and (400) [52–55]. The observed XRD pattern was also consistent with the standard CeO_2 crystal (JCPDS-No-34-0394). The average crystallite size of nanoceria synthesized from the BL extract was determined using Scherrer's formula (Equation (2)):

$$D = \frac{0.9\lambda}{\beta cos\theta} \quad (2)$$

where D is the crystalline size, λ is the wavelength of X-ray used (CuKα radiation 1.54 Å), β represents the full line width at the half maximum of the peak, and θ is the Bragg angle. The calculated average crystalline diameter of CeO_2 NPs was 24.46 nm.

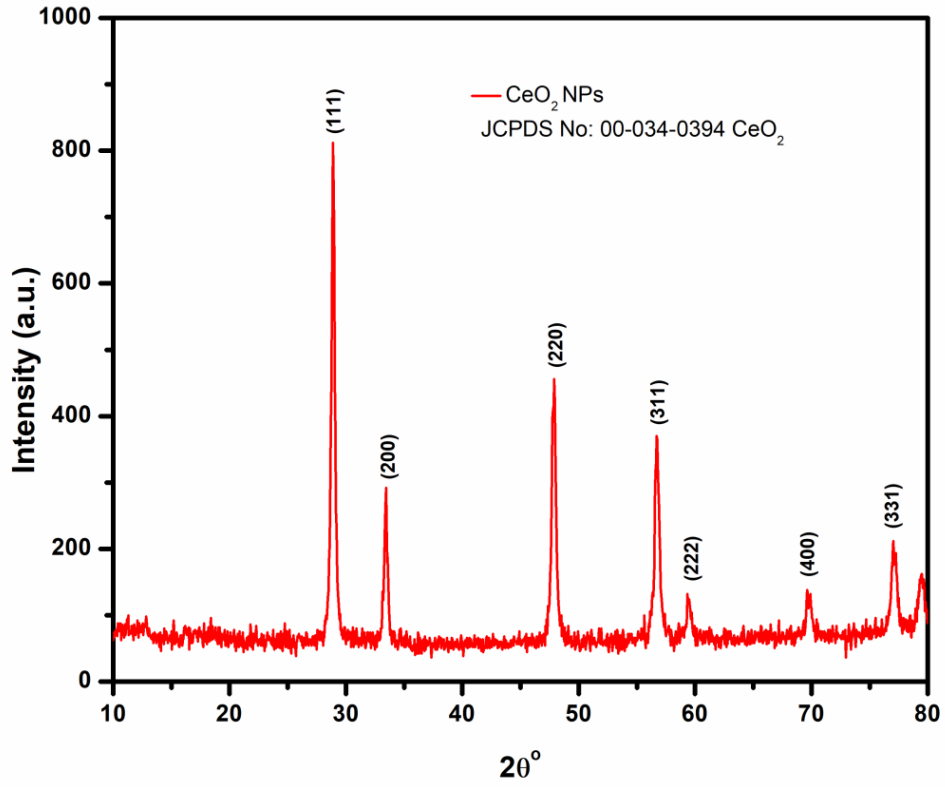

Figure 2. XRD analysis of biosynthesized CeO_2 NPs made from BL extract.

3.2.3. FT-IR Analysis

FT-IR is a crucial technique for identifying and characterizing a material since it offers information on a molecule's vibrational modes of motion. The infrared spectrum of an organic compound provide a unique fingerprint that can be easily distinguished from the absorption patterns of all other compounds. The FT-IR spectrums of CeO_2 NPs (Figure 3a) and BL aqueous extract (Figure 3b) were studied, as illustrated in Figure 3. The spectral peak at 3291 cm^{-1} is due to O–H stretching vibration of phenolic compounds while the stretching vibration of C–H band at 2938.72 cm^{-1} could be ascribed to the presence of CH_2 and CH_3 groups [56]. The carbonyl group has an absorption peak at 1613 cm^{-1}, which can be attributed to the presence of a deformed aromatic ring, amino acids, and flavonoids, while primary amine groups and the -C-H stretching mode have a band at 1448 cm^{-1} [56,57]. The stretching band at 1235 cm^{-1} belongs to the C-O stretching vibration of the ester group. The characteristic C-N stretching vibration mode of amines, which can be found in proteins and enzymes, is responsible for the absorption band at 1017 cm^{-1} [58].

The characteristic absorption of polysaccharides, especially with a peak at 832 cm^{-1}, belongs to the characteristic peak of α-glucose [56]. On the other hand, the phytoactive compounds were either shifted or quenched during the reduction and stabilization of the CeO_2 NPs, as illustrated in Figure 3a, which corresponds to the FTIR spectrum of the BL-synthesized CeO_2 NPs. The broad peaks at 3371 cm^{-1} indicate the presence of O-H vibration of hydroxyl group which is slightly shifted. The band at 2922 cm^{-1} completely disappeared in the annealed sample most likely because of the higher temperature [59]. Similarly, the peaks in CeO_2 NPs present at 1613 cm^{-1}, 1500 cm^{-1}, 1334 cm^{-1}, and 1153 cm^{-1}, which were assigned to C=O, C-H, and C-N groups of phytochemicals present in the BL leaf extract were also shifted. The band near 467 cm^{-1} was attributed to Ce-O stretching vibration, and a similar low wavenumber for Ce-O vibration has previously been reported for nanoceria. [52,54].

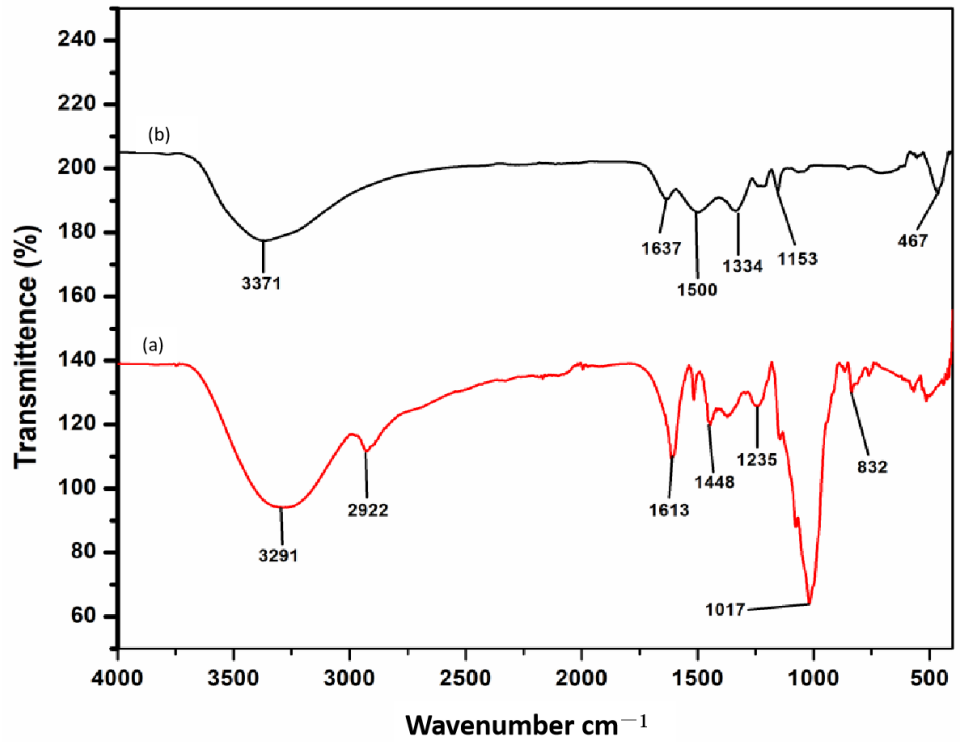

Figure 3. FTIR absorption spectral analysis. (a) *B. cylindrica* leaves-synthesized CeO_2 NPs after complete bioreduction. (b) *B. cylindrica* leaf extract before bioreduction.

3.2.4. TEM Analysis

TEM analysis of the CeO_2 NPs generated via BL aqueous extract is displayed in Figure 4a,b. The TEM micrographs of the produced nanoparticles indicate a heterogeneous morphology of CeO_2 NPs with the formation of spherical and cubic-like structures with an average diameter in the 40–60 nm range. The selected area diffraction (SAED) pattern of CeO_2 NPS synthesized using BL aqueous extract (Figure 4c) was consistent with the XRD study demonstrating the cubic fluorite structure of CeO_2 NPs.

3.2.5. Dynamic Light Scattering (DLS) and Zeta Potential

CeO_2 NPs synthesized using BL aqueous extract revealed a hydrodynamic size of 56.30 ± 33.26 nm using DLS (Figure 5a) with a polydispersity index of 0.280. The zeta potential was found to be −20.7 mV (Figure 5b) at pH 7.5, indicating that the nanoparticles' surfaces are negatively charged and that they are uniformly distributed in the medium. The negative value confirmed the nanoparticle repulsion and demonstrated their stability in the homogeneous medium.

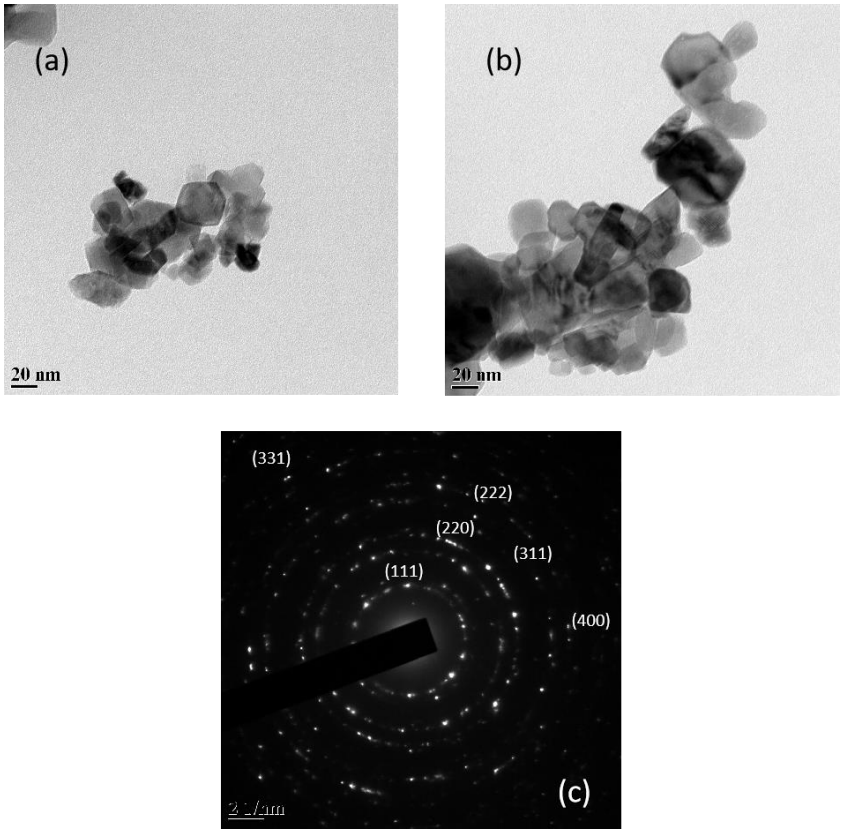

Figure 4. (**a**,**b**) TEM images of CeO_2 nanoparticles biosynthesized using the BL extract at a magnification of 20 nm. (**c**) SAED pattern of synthesized CeO_2 nanoparticles.

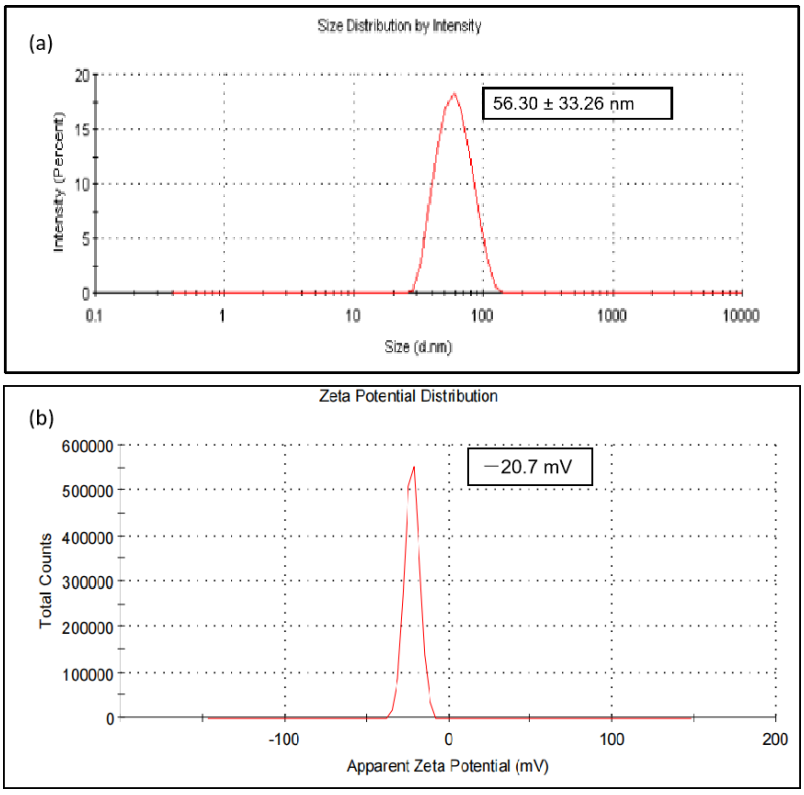

Figure 5. (**a**) Hydrodynamic size distribution of CeO_2 NPs synthesized using BL extract; (**b**) zeta(ζ) potential of synthesized CeO_2 NPs at pH 7.5.

3.2.6. Energy Dispersive X-ray Spectra (EDS) of CeO_2 NPs

EDS of CeO_2 NPs synthesized using BL aqueous extract displayed a significant amount of cerium and oxygen peaks (Figure 6). The presence of elemental cerium peaks existed between 4 and 5 keV, while the peaks of oxide displayed in the range of 0.5–1 keV [60]. The energy peak that appears at approximately 1.4 KeV correspond to the aluminum of the sample holder. The energy peak at 0.3 KeV corresponds to peak of carbon.

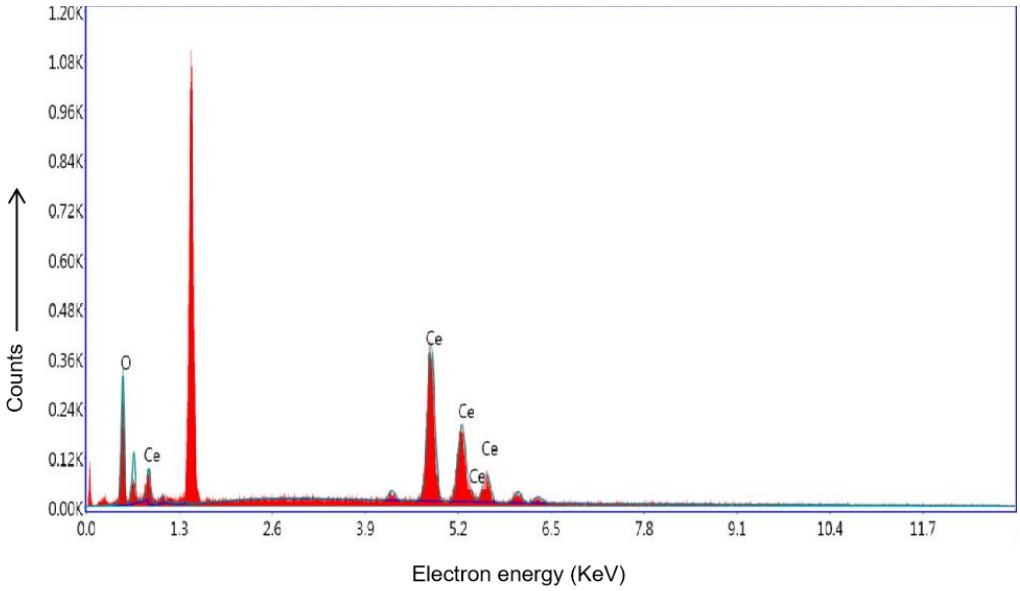

Figure 6. EDS of BL-synthesized CeO_2 NPs.

3.3. Mosquito Larvicidal Activity

To determine the level of effectiveness, early fourth instar *Ae. aegypti* larvae were exposed to varying concentrations of BL extract and biosynthesized CeO_2 NPs for a duration of 24 h. The mortality rate of mosquito larvae increased in proportion to the increasing concentration of plant extracts and CeO_2 nanoparticles. The BL aqueous extract alone was less harmful to *Ae. aegypti* larvae than the BL-synthesized CeO_2 NPs. CeO_2 NPs at a concentration of 70 µg/mL caused 100% mortality, with LC_{50} and LC_{90} values of 46.28 and 64.62 µg/mL, respectively, while at 2500 µg/mL, the BL extract demonstrated 100% mortality with LC_{50} and LC_{90} values of 1258.04 and 2250.03 µg/mL, respectively (Table 2). The control group's mosquito larvae did not show any signs of toxicity, and the $\chi 2$ value revealed a statistically significant difference in BL extract and CeO_2 NPs at a level of $p < 0.05$. The results show that CeO_2 NPs have almost 27 times the larvicidal potential of the BL extract.

3.4. Enzyme Activity

3.4.1. Acetylcholinesterase (AChE) Activity

The AChE enzyme was used as a potential biomarker to evaluate neurotoxicity in vitro [61]. In view of this, we looked into how BL extract and CeO_2 NPs affect AChE activity in *Ae. aegypti* fourth instar larvae. When compared to the control value of 3.58 µM ACT hydrolyzed/min/mg protein of homogenate, the AChE activity of larvae exposed to BL extract and CeO_2 NPs for 24 h was greatly reduced to 2.21 µM ACT hydrolyzed/min/mg protein and 1.88 µM ACT hydrolyzed/min/mg protein, respectively (Figure 7).

Table 2. Larvicidal toxicity of *B. cylindrica* leaves extract and synthesized CeO_2 NPs against the dengue vector *Ae. aegypti*.

Treatment	Concentration (µg/mL)	24 h Mortality (%) ± SE	LC50 (µg/mL)	LCL–UCL	LC90 (µg/mL)	LCL–UCL	χ^2 (d.f.)
B. cylindrica aqueous extract	250	4.58 ± 0.96	1258.04	583.87–1574.89	2250.03	1787.97–5310.37	16.73 * (4) (p = 0.002)
	500	13.75 ± 1.25					
	750	22.91 ± 1.29					
	1000	38.33 ± 2.16					
	1500	56.25 ± 2.39					
	2000	84.58 ± 2.25					
	2500	100 ± 0.00					
CeO_2 NPs	10	6.66 ± 0.71	46.28	17.38–53.20	64.62	56.16–179.54	17.06 * (4) (p = 0.002)
	20	16.25 ± 1.25					
	30	23.75 ± 1.08					
	40	41.25 ± 1.95					
	50	57.50 ± 1.44					
	60	83.75 ± 1.64					
	70	100 ± 0.00					

There was no mortality in the control group. LC_{50}—the amount that kills 50% of the organisms that are exposed to it; LC_{90}—the amount that kills 90% of the organisms that are exposed to it; χ2—chi-square; d.f.—degrees of freedom; (*) significance at ($p \leq 0.05$); LCL—lower confidential limits; UCL—upper confidential limits.

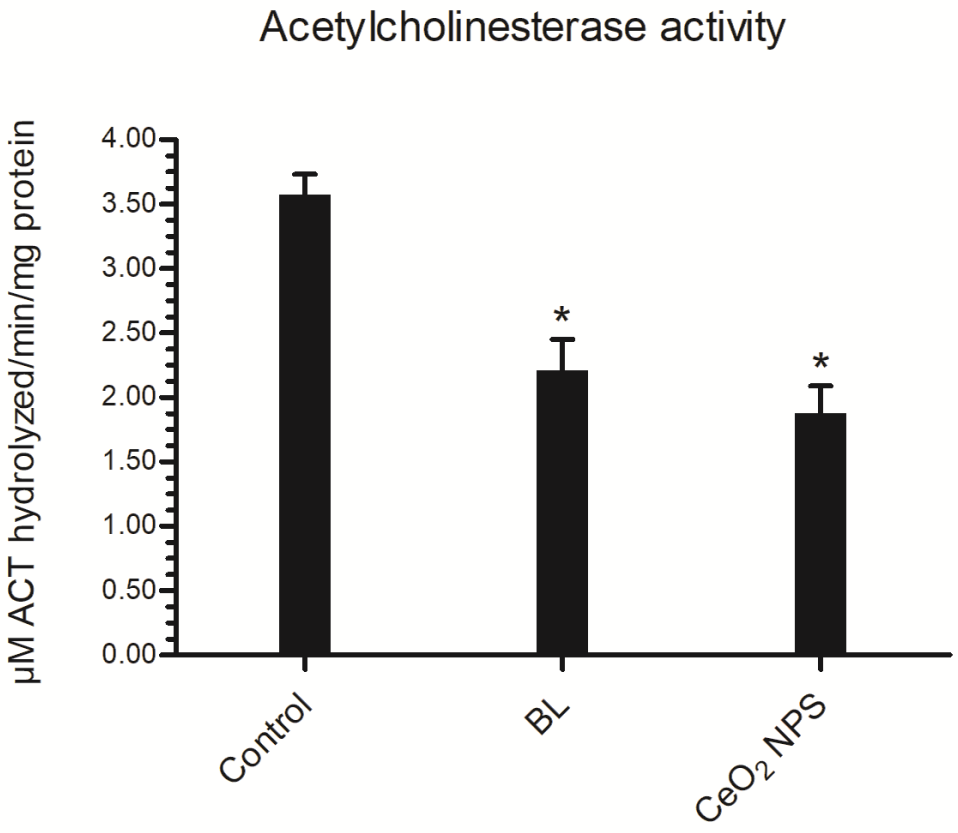

Figure 7. *Ae. aegypti* larvae AChE activity at LC_{50} concentrations of BL aqueous extract and BL-synthesized CeO_2 NPs. Results are provided as mean ± SEM (n = 3). * $p < 0.05$ (ANNOVA, Tukey's HSD test) indicate a significant difference from the control.

3.4.2. Glutathione S-Transferase (GST) Activity

The vast majority of the time, GST plays a substantial part in the removal of both endogenous and exogenous compounds. In this study, the BL extract resulted in a marginal improvement in GST activity (0.41 µM CDNB conjugated/min/mg protein), whereas synthesized CeO_2 NPs resulted in a significant reduction in GST activity (0.32 µM CDNB conjugated/min/mg protein) in comparison to the control (0.37 µM CDNB conjugated/min/mg protein) (Figure 8).

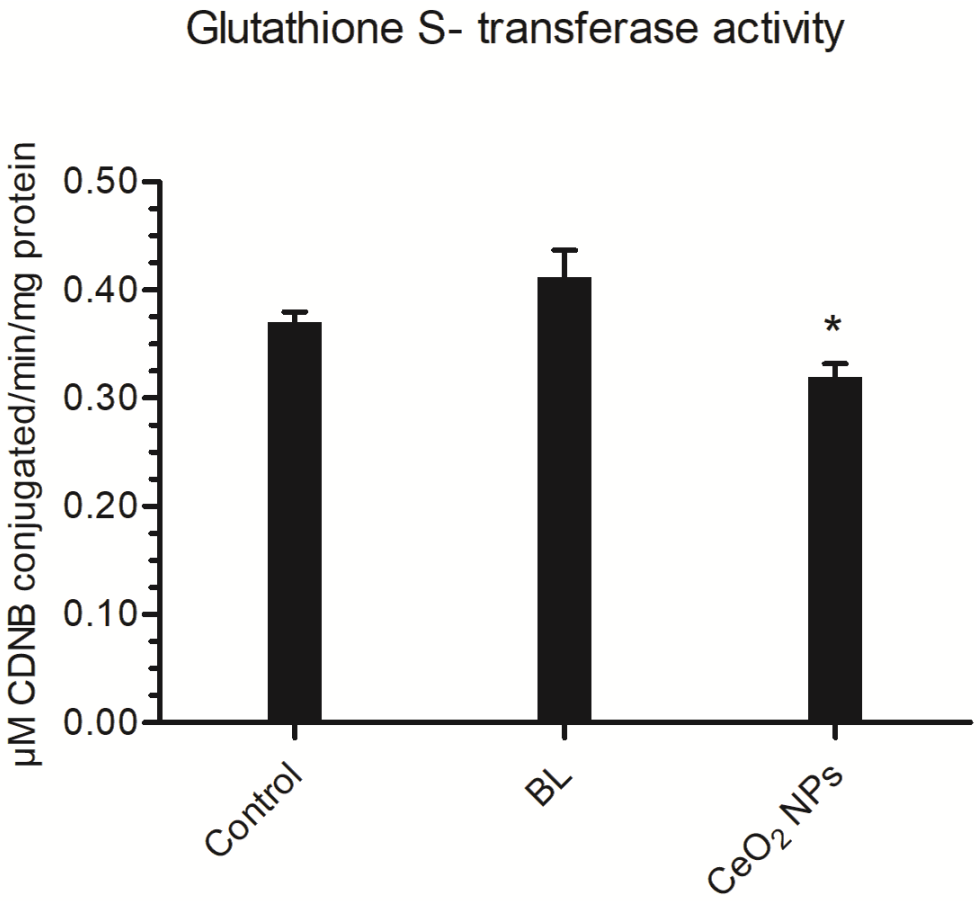

Figure 8. *Ae. aegypti* larvae GST activity at LC_{50} concentrations of BL aqueous extract and BL-synthesized CeO_2 NPs. Results are provided as mean ± SEM ($n = 3$). * $p < 0.05$ (ANNOVA, Tukey's HSD test) indicate a significant difference from the control.

4. Discussion

In response to the herbivore and microbe selection pressures, many marine plants synthesize a varied range of chemically different secondary metabolites, some of which are now identified as insecticides. The bioactivity of phytochemicals against mosquito larvae varies greatly depending on plant species, plant sections, plant age, extraction solvent, and mosquito species [62]. Aqueous extract of *B. cylindrica* showed the presence of alkaloids, flavonoids, terpenoids, tannins, saponins, proteins, phenolic compounds, and reducing sugars, which may have contributed in the larvicidal activity [63]. The current study also describes the synthesis of CeO_2 NPs utilizing *B. cylindrica* leaves extract. The color change is a visual indication of the formation of cerium nanoparticles. As a result, this confirmed that the BL extract plays an important role as an oxidizing agent. Furthermore, it works by maintaining the growth and controlling the size of nanoparticles, so it also serves as a capping agent. When CeO_2 NPs were synthesized using *Moringa oleifera* leaf extract, similar observations were obtained [64].

The UV–visible spectra of the synthesized NPs revealed that the maximum absorbance occurred at 303 nm with the band gap of 3.17 eV. Pop et al. [49] got a similar band absorption

peak from CeO_2 NPs. This is related to the intrinsic band-gap, which can be seen when electrons move from the valance band to the conduction band. Researchers have found that a band with a wavelength of 302 nm is produced when a charge transfer from O (2p) to Ce (4f) occurs in cerium oxide. [33,50,65,66]. Biomolecules present in the BL aqueous extract showed strong spectral peaks due to O–H, C–H, primary amine groups, and -C-O, C-N stretching modes. FTIR spectrum of CeO_2 NPs showed that the phytoactive compounds such as terpenes, polysaccharides, flavonoids, and amino acids present in the BL aqueous extract may have contributed to stabilizing the CeO_2 NPs [56–58,67]. In the current study, the stretching frequency of Ce-O was seen at 467 cm^{-1}, thereby confirming the synthesis of CeO_2 NPs [33]. As a result, the vibration at 467 cm^{-1} is regarded as a typical phononic mode for cubic CeO_2 NPs. A similar characteristic peak was observed in CeO_2 NPs synthesized using aerial parts of *Prosopis farcta* [54]. Whereas the intensity of copious biomolecules decreased due to the annealing of the CeO_2 sample at a higher temperature.

TEM micrographs and DLS suggest that the generated nanoparticles clearly show a mixed morphology of CeO_2 NPs with the formation of spherical and cubic-like structures with an average size in the range of 40–60 nm in diameter, which is confirmed with XRD and SAED patterns. The mean crystalline size of the ordered CeO_2 NPs has been estimated to be around 24.46 nm. The EDS graph indicated the presence of cerium and oxygen in the sample. The surface charge and stability of the BL-synthesized CeO_2 NPs revealed the zeta potential value of −20.7 mV, indicating the surface charge of the synthesized nanoparticles. The negative charge potential value could be measured because of the reducing agent for the flavonoid and polyphenolic constituents present in the leaf extract of *B. cylindrica,* which reveals the presence of gross electrostatic forces with the green synthesized CeO_2 NPs. Similar outcomes were also obtained with CeO_2 NPs made from *Aloe vera* leaf extract, which had a zeta potential of −12 mV [68]. Because of this, it has been hypothesized that the nanoparticles have a negatively charged surface that is dispersed throughout the medium because of the negatively charged functional groups from the plant compounds, which may have contributed to the colloidal stability [69]. Overall, the BL aqueous extract can be utilized for the formation of stable cubic fluorite structures of CeO_2 NPs using phytochemicals present in the BL aqueous extracts as oxidizing and capping agents.

CeO_2 NPs synthesized from the BL aqueous extract displayed 100% mortality at 70 µg/mL with an LC_{50} value of 46.28 µg/mL. The CeO_2 NPs showed an almost 27-fold higher mortality rate compared to BL extract treatment alone (1258.04 µg/mL). Similarly, 24 h of exposure to CeO_2 NPs generated using culture filtrate of *Aspergillus niger* resulted in 100% mortality of first instar larvae of *Ae. aegypti* [70]. The obtained findings indicate that the CeO_2 NPs may be interfering with membrane permeability, resulting in cell death, but the precise mechanism is unknown. Recently, it was discovered that when NPs interact with larval cell membranes, the cells lose their integrity, and the larvae die [71]. Furthermore, the tested compounds inhibit the activity of AChE, an enzyme involved in the hydrolysis of acetylcholine, at nerve synapses and neuromuscular junctions.

Acetylcholinesterase (AChE) enzyme is the primary target of organophosphorous (OP) and carbamate insecticides in insect pests, and it is encoded by the AChE gene. One of the most important resistance mechanisms in insect pests is mutations in this gene [72]. Therefore, AChE activity was carried out on survived larvae to understand the mechanism of larvicidal potency of the BL aqueous extract and synthesized CeO_2 NPs. Prior studies have shown that certain mangrove plants, specifically *Avicennia marina*, *Rhizophora annamalayana*, *Rhizophora apiculata*, *Rhizophora mucronata*, and *B. cylindrica*, can reduce the level of acetylcholinesterase (AChE) activity in mosquito larvae by as much as 50% [73]. Plant compounds can alter larvae's digestive, respiratory, and neurological systems, according to previous studies [74]. The inhibition of the AChE enzyme causes the muscles to remain contracted, which ultimately leads to paralysis and, in some cases, death [75]. In the current work, BL plant extract and synthesized CeO_2 NPs reduced AChE activity in *Ae. aegypti* larvae by nearly 38% and 47%, respectively, at their LC_{50} concentrations. Thus, in the current investigation, AChE inhibition would have likely

hampered the larvae's ability to breathe freely, resulting in mortality. Thus, the results of the current experiments indicate that CeO_2 NPs synthesized from the BL extract have some neurotoxic potential. Another important enzyme, GSTs have been known to be involved in the detoxification of xenobiotic compounds in general. Insecticides affect this detoxification enzyme in target insect tissues and organs. Certain chemicals can increase or decrease GST activity [76]. In the current experiments, *Ae. aegypti* larvae treated with BL aqueous extract showed a 9.75% increase in GST activity, indicating an effort to detoxify plant compounds. However, CeO_2 NPs may have caused oxidative stress damage to larval tissues, as evidenced by a 13.51% decrease in GST activity, suggesting that the NPs may be engaged in a redox reaction [77–79]. An aqueous extract from *Lumnizera racemosa* flower buds and zinc oxide nanorods synthesized from them showed a similar reduction in GST activity in *Ae. aegypti* larvae [80]. As a result, the blockage or stimulation of these enzymes by different metabolites from plants or NPs might result in metabolic disparities, which in turn can lead to growth retardation and the induction of mortality in mosquito larvae [81,82]. Therefore, it is possible to draw the conclusion that BL-synthesized CeO_2 NPs in the current study damage mosquito larval cells by interfering with the AChE and GST enzymes.

5. Conclusions

This is the first work to report on the green production of CeO_2 NPs by utilizing *B. cylindrica* leaves. UV–Vis spectrophotometry, TEM, XRD, FTIR, and EDX analysis results support the successful biosynthesis of the CeO_2 NPs. The crystalline and cubic CeO_2 NPs generated had an average size of 40–60 nm. The current study found that CeO_2 NPs are simple to make and may be used at low doses to significantly reduce populations of the dengue vector, *Ae. aegypti*, with an LC_{50} of 46.28µg/mL. Furthermore, CeO_2 NPs reduce the activity of enzymes in *Ae. aegypti* larvae, resulting in lower AChE and GST activity, which are responsible for signal transmission and xenobiotic resistance. The study indicates that CeO_2 NPs can be considered as effective nanobiopesticides in the future to inhibit the dengue vector, *Ae. aegypti* larvae.

Author Contributions: Conceptualization, P.P.D. and V.R.S.; methodology, P.P.D., V.R.S. and A.K.M.; experiments, P.P.D. and V.R.S.; writing—original draft preparation, P.P.D., V.R.S. and A.K.M.; writing—review and editing, P.P.D., V.R.S. and A.K.M. All authors have read and agreed to the published version of the manuscript.

Funding: This research did not receive any specific grant from funding agencies in the public, commercial, or not-for-profit sectors.

Institutional Review Board Statement: Not applicable.

Informed Consent Statement: Not applicable.

Data Availability Statement: Not applicable.

Acknowledgments: Authors are thankful to the Department of Life Sciences, Department of Chemistry, National Centre for Nanoscience and Nanotechnology, University of Mumbai; IIT Bombay (SAIF) for Accessing Instrument Facility. Department of Zoonosis, Haffkine Institute for Training Research and Testing Mumbai, Maharashtra, for the identification of mosquito species.

Conflicts of Interest: The authors declare no conflict of interest.

References

1. Taubes, G. Malaria Parasite Outwits the Immune System. *Science* **2000**, *290*, 435. [CrossRef] [PubMed]
2. Murugan, K.; Murugan, P.; Noortheen, A. Larvicidal and repellent potential of Albizzia amara Boivin and Ocimum basilicum Linn against dengue vector, *Aedes aegypti* (Insecta: Diptera: Culicidae). *Bioresour. Technol.* **2007**, *98*, 198–201. [CrossRef] [PubMed]
3. Vasudevan, K.; Malarmagal, R.; Charulatha, H.; Saraswatula, V.L.; Prabakaran, K. Larvicidal effects of crude extracts of dried ripened fruits of Piper nigrum against *Culex quinquefasciatus* larval instars. *J. Vector Borne Dis.* **2009**, *46*, 153.

4. Kamaraj, C.; Bagavan, A.; Rahuman, A.A.; Zahir, A.A.; Elango, G.; Pandiyan, G. Larvicidal potential of medicinal plant extracts against *Anopheles subpictus Grassi* and *Culex tritaeniorhynchus Giles* (Diptera: Culicidae). *Parasitol. Res.* **2009**, *104*, 1163–1171. [CrossRef] [PubMed]
5. Goncalvez, A.P.; Engle, R.E.; St. Claire, M.; Purcell, R.H.; Lai, C.J. Monoclonal antibody-mediated enhancement of dengue virus infection in vitro and in vivo and strategies for prevention. *Proc. Natl. Acad. Sci. USA* **2007**, *104*, 9422–9427. [CrossRef]
6. Wiratsudakul, A.; Suparit, P.; Modchang, C. Dynamics of Zika virus outbreaks: An overview of mathematical modeling approaches. *PeerJ* **2018**, *6*, e4526. [CrossRef] [PubMed]
7. WHO. *Dengue: Guidelines for Diagnosis, Treatment, Prevention and Control*; WHO Library: Geneva, Switzerland, 2009; pp. 10–12.
8. World Health Organization. Available online: https://www.who.int/srilanka/news/detail/08-07-2019-preventive-action-is-vital-to-curtail-dengue-outbreaks-in-sri-lanka (accessed on 1 February 2023).
9. Weaver, S.C.; Reisen, W.K. Present and future arboviral threats. *Antivir. Res.* **2010**, *85*, 328–345. [CrossRef] [PubMed]
10. Wilke, A.B.; Vasquez, C.; Carvajal, A.; Ramirez, M.; Cardenas, G.; Petrie, W.D.; Beier, J.C. Effectiveness of adulticide and larvicide in controlling high densities of *Aedes aegypti* in urban environments. *PLoS ONE* **2021**, *16*, e0246046. [CrossRef]
11. Subahar, R.; Aulia, A.P.; Yulhasri, Y.; Felim, R.R.; Susanto, L.; Winita, R.; El Bayani, G.F.; Adugna, T. Assessment of susceptible *Culex quinquefasciatus* larvae in Indonesia to different insecticides through metabolic enzymes and the histopathological midgut. *Heliyon* **2022**, *8*, e12234. [CrossRef]
12. De Castro, B.M.; De Jaeger, X.; Martins-Silva, C.; Lima, R.D.F.; Amaral, E.; Menezes, C.; Lima, P.; Neves, C.M.L.; Pires, R.G.; Gould, T.W.; et al. The vesicular acetylcholine transporter is required for neuromuscular development and function. *Mol. Cell. Biol.* **2009**, *29*, 5238–5250. [CrossRef]
13. Melo-Santos, M.; Varjal-Melo, J.; Araújo, A.; Gomes, T.; Paiva, M.; Regis, L.; Furtado, A.; Magalhaes, T.; Macoris, M.; Andrighetti, M.; et al. Resistance to the organophosphate temephos: Mechanisms, evolution and reversion in an *Aedes aegypti* laboratory strain from Brazil. *Acta Trop.* **2010**, *113*, 180–189. [CrossRef] [PubMed]
14. Azizullah, A.; Rehman, Z.U.; Ali, I.; Murad, W.; Muhammad, N.; Ullah, W.; Häder, D.P. Chlorophyll derivatives can be an efficient weapon in the fight against dengue. *Parasitol. Res.* **2014**, *113*, 4321–4326. [CrossRef] [PubMed]
15. Saddhe, A.A.; Jamdade, R.A.; Kumar, K. Evaluation of multilocus marker efficacy for delineating mangrove species of West Coast India. *PLoS ONE* **2017**, *12*, e0183245. [CrossRef]
16. Revathi, P.; Jeyaseelansenthinath, T.; Thirumalaikolundhusubramaian, P. Preliminary Phytochemical Screening and GCMS Analysis of Ethanolic Extract of Mangrove Plant—*Bruguiera cylindrica* (Rhizho) L. *Int. J. Pharmacogn. Phytochem. Res.* **2014**, *6*, 729–740.
17. Nithyamol Kalappurakkal, V.; Bhattacharya, D.; Chakravarty, S.; Venkata Uppuluri, M. Isolation, synthesis and AC hE inhibitory potential of some novel cinnamyl esters of taraxerol, the major metabolite of the Mangrove *Bruguiera cylindrica*. *Chem. Biodivers.* **2018**, *15*, e1800008. [CrossRef]
18. Bobbarala, V.; Vadlapudi, V.R.; Naidu, C.K. Antimicrobial potentialities of mangrove plant Avicennia marina. *J. Pharm. Res.* **2009**, *2*, 1019–1021.
19. Dahibhate, N.L.; Saddhe, A.A.; Kumar, K. Mangrove plants as a source of bioactive compounds: A review. *Nat. Prod. J.* **2019**, *9*, 86–97. [CrossRef]
20. Dahibhate, N.L.; Roy, U.; Kumar, K. Phytochemical screening, antimicrobial and antioxidant activities of selected mangrove species. *Curr. Bioact. Compd.* **2020**, *16*, 152–163. [CrossRef]
21. Krishnamoorthy, M.; Sasikumar, J.M.; Shamna, R.; Pandiarajan, C.; Sofia, P.; Nagarajan, B. Antioxidant activities of bark extract from mangroves, *Bruguiera cylindrica* (L.) Blume and Ceriops decandra Perr. *Indian J. Pharmacol.* **2011**, *43*, 557.
22. Premanathan, M.; Kathiresan, K.; Nakashima, H. Mangrove halophytes: A source of antiviral substances. *South Pac. Study* **1999**, *19*, 49–57.
23. Murugan, K.; Dinesh, D.; Paulpandi, M.; Althbyani, A.D.M.; Subramaniam, J.; Madhiyazhagan, P.; Wang, L.; Suresh, U.; Kumar, P.M.; Mohan, J.; et al. Nanoparticles in the fight against mosquito-borne diseases: Bioactivity of *Bruguiera cylindrica*—Synthesized nanoparticles against dengue virus DEN-2 (in vitro) and its mosquito vector Aedes aegypti (Diptera: Culicidae). *Parasitol. Res.* **2015**, *114*, 4349–4361. [CrossRef]
24. Benelli, G. Research in mosquito control: Current challenges for a brighter future. *Parasitology research* **2015**, *114*, 2801–2805. [CrossRef] [PubMed]
25. Pandey, A.; Mishra, A.K. Immunomodulation, Toxicity, and Therapeutic Potential of Nanoparticles. *BioTech* **2022**, *11*, 42. [CrossRef] [PubMed]
26. Miao, J.J.; Wang, H.; Li, Y.R.; Zhu, J.M.; Zhu, J.J. Ultrasonic-induced synthesis of CeO_2 nanotubes. *J. Cryst. Growth* **2005**, *281*, 525–529. [CrossRef]
27. Thakur, S.; Patil, P. Rapid synthesis of cerium oxide nanoparticles with superior humidity-sensing performance. *Sens. Actuators B Chem.* **2014**, *194*, 260–268. [CrossRef]
28. Khan, S.B.; Faisal, M.; Rahman, M.M.; Jamal, A. Exploration of CeO_2 nanoparticles as a chemi-sensor and photo-catalyst for environmental applications. *Sci. Total Environ.* **2011**, *409*, 2987–2992. [CrossRef] [PubMed]
29. Patil, S.; Sandberg, A.; Heckert, E.; Self, W.; Seal, S. Protein adsorption and cellular uptake of cerium oxide nanoparticles as a function of zeta potential. *Biomaterials* **2007**, *28*, 4600–4607. [CrossRef]

30. Zhang, P.; Ma, Y.; Zhang, Z.; He, X.; Zhang, J.; Guo, Z.; Tai, R.; Zhao, Y.; Chai, Z. Biotransformation of ceria nanoparticles in cucumber plants. *ACS Nano* **2012**, *6*, 9943–9950. [CrossRef]
31. Thill, A.; Zeyons, O.; Spalla, O.; Chauvat, F.; Rose, J.; Auffan, M.; Flank, A.M. Cytotoxicity of CeO2 nanoparticles for Escherichia coli. Physico-chemical insight of the cytotoxicity mechanism. *Environ. Sci. Technol.* **2006**, *40*, 6151–6156. [CrossRef]
32. Panahi-Kalamuei, M.; Alizadeh, S.; Mousavi-Kamazani, M.; Salavati-Niasari, M. Synthesis and characterization of CeO_2 nanoparticles via hydrothermal route. *J. Ind. Eng. Chem.* **2015**, *21*, 1301–1305. [CrossRef]
33. Arumugam, A.; Karthikeyan, C.; Hameed, A.S.H.; Gopinath, K.; Gowri, S.; Karthika, V. Synthesis of cerium oxide nanoparticles using *Gloriosa superba* L. leaf extract and their structural, optical and antibacterial properties. *Mater. Sci. Eng. C* **2015**, *49*, 408–415. [CrossRef] [PubMed]
34. Charbgoo, F.; Ahmad, M.B.; Darroudi, M. Cerium oxide nanoparticles: Green synthesis and biological applications. *Int. J. Nanomed.* **2017**, *12*, 1401. [CrossRef] [PubMed]
35. Aboyewa, J.A.; Sibuyi, N.R.; Meyer, M.; Oguntibeju, O.O. Green synthesis of metallic nanoparticles using some selected medicinal plants from southern africa and their biological applications. *Plants* **2021**, *10*, 1929. [CrossRef]
36. Bharadwaj, K.K.; Rabha, B.; Pati, S.; Sarkar, T.; Choudhury, B.K.; Barman, A.; Bhattacharjya, D.; Srivastava, A.; Baishya, D.; Edinur, H.A.; et al. Green synthesis of gold nanoparticles using plant extracts as beneficial prospect for cancer theranostics. *Molecules* **2021**, *26*, 6389. [CrossRef] [PubMed]
37. Shah, M.; Fawcett, D.; Sharma, S.; Tripathy, S.K.; Poinern, G.E.J. Green synthesis of metallic nanoparticles via biological entities. *Materials* **2015**, *8*, 7278–7308. [CrossRef] [PubMed]
38. Gawali, P.; Jadhav, B.L. Antioxidant activity and antioxidant phytochemical analysis of mangrove species *Sonneratia alba* and *Bruguiera cylindrica*. *Asian J. Microbiol. Biotechnol. Environ. Sci.* **2011**, *13*, 257–261.
39. Ranjana, B.L.; Jadhav, B.; Dhavan, P.; Patel, P. In vitro antidiabetic activity and phytochemical analysis of *Lumnitzera racemosa* leaves. *Int. Res. J. Pharm.* **2010**, *10*, 220–227.
40. Kumar, S.; Warikoo, R.; Wahab, N. Larvicidal potential of ethanolic extracts of dried fruits of three species of peppercorns against different instars of an Indian strain of dengue fever mosquito, *Aedes aegypti* L. (Diptera: Culicidae). *Parasitol. Res.* **2010**, *107*, 901–907. [CrossRef]
41. Weger-Lucarelli, J.; Rückert, C.; Chotiwan, N.; Nguyen, C.; Luna, S.M.G.; Fauver, J.R.; Foy, B.D.; Perera, R.; Black, W.C.; Kading, R.C.; et al. Vector competence of American mosquitoes for three strains of Zika virus. *PLoS Negl. Trop. Dis.* **2016**, *10*, e0005101. [CrossRef]
42. Finlayson, C.; Saingamsook, J.; Somboon, P. A simple and affordable membrane-feeding method for *Aedes aegpyti* and *Anopheles minimus* (Diptera: Culicidae). *Acta Trop.* **2015**, *152*, 245–251. [CrossRef]
43. World Health Organization. *Safety of Pyrethroids for Public Health Use*; No. WHO/CDS/WHOPES/GCDPP/2005.10; World Health Organization: Geneva, Switzerland, 2005.
44. Napoleão, T.H.; Pontual, E.V.; Lima, T.D.A.; Santos, N.D.D.L.; Sá, R.A.; Coelho, L.C.B.B.; Navarro, D.M.D.A.F.; Paiva, P.M.G. Effect of *Myracrodruon urundeuva* leaf lectin on survival and digestive enzymes of *Aedes aegypti* larvae. *Parasitol. Res.* **2012**, *110*, 609–616. [CrossRef] [PubMed]
45. Bradford, M.M. A rapid and sensitive method for the quantitation of microgram quantities of protein utilizing the principle of protein-dye binding. *Anal. Biochem.* **1976**, *72*, 248–254. [CrossRef] [PubMed]
46. Ellman, G.L.; Courtney, K.D.; Andres, V., Jr.; Featherstone, R.M. A new and rapid colorimetric determination of acetylcholinesterase activity. *Biochem. Pharmacol.* **1961**, *7*, 88–95. [CrossRef]
47. Ikezawa, H.; Taguchi, R. [84] Phosphatidylinositol-specific phospholipase C from *Bacillus cereus* and *Bacillus thuringiensis*. *Methods Enzymol.* **1981**, *71*, 731–741.
48. Habig, W.H.; Pabst, M.J.; Jakoby, W.B. Glutathione S-transferases: The first enzymatic step in mercapturic acid formation. *J. Biol. Chem.* **1974**, *249*, 7130–7139. [CrossRef] [PubMed]
49. Kim, R.; Boyd, M. Japanese consumers' acceptance of genetically modified (GM) Food: An ordered probit analysis. *J. Food Prod. Mark.* **2006**, *12*, 45–57. [CrossRef]
50. Pop, O.L.; Mesaros, A.; Vodnar, D.C.; Suharoschi, R.; Tăbăran, F.; Mageruşan, L.; Tódor, I.S.; Diaconeasa, Z.; Balint, A.; Ciontea, L.; et al. Cerium oxide nanoparticles and their efficient antibacterial application in vitro against gram-positive and gram-negative pathogens. *Nanomaterials* **2020**, *10*, 1614. [CrossRef]
51. Gu, H.; Soucek, M.D. Preparation and characterization of monodisperse cerium oxide nanoparticles in hydrocarbon solvents. *Chem. Mater.* **2007**, *19*, 1103–1110. [CrossRef]
52. Sharmila, G.; Muthukumaran, C.; Saraswathi, H.; Sangeetha, E.; Soundarya, S.; Kumar, N.M. Green synthesis, characterization and biological activities of nanoceria. *Ceram. Int.* **2019**, *45*, 12382–12386. [CrossRef]
53. Elaziouti, A.; Laouedj, N.; Bekka, A.; Vannier, R.N. Preparation and characterization of p–n heterojunction $CuBi_2O_4/CeO_2$ and its photocatalytic activities under UVA light irradiation. *J. King Saud Univ. Sci.* **2015**, *27*, 120–135. [CrossRef]
54. Miri, A.; Sarani, M. Biosynthesis, characterization and cytotoxic activity of CeO_2 nanoparticles. *Ceram. Int.* **2018**, *44*, 12642–12647. [CrossRef]

55. Arul, N.S.; Mangalaraj, D.; Han, J.I. Facile hydrothermal synthesis of CeO_2 nanopebbles. *Bull. Mater. Sci.* **2015**, *38*, 1135–1139. [CrossRef]
56. Baseri, M.K.; Baker, S. Identification of cellular components of medicinal plants using FTIR. *Rom. J. Biophys.* **2011**, *21*, 277–284.
57. Silva, J.P.; Méndez, G.L.; Lombana, J.; Marrugo, D.G.; Correa-Turizo, R. Physicochemical Characterization of Spent Coffee Ground (*Coffea arabica* L.) and its Antioxidant Evaluation. *Adv. J. Food Sci. Technol.* **2018**, *16*, 220–225. [CrossRef]
58. Al, R.N.; Al-Haidari, K.S. Environmental friendly synthesis of silver nanoparticles using leaf extract of Mureira Tree (*Azadirachta indica*) cultivated in Iraq and efficacy the antimicrobial activity. *J. Nat. Sci. Res.* **2016**, *6*, 2224–3186.
59. Bakkiyaraj, R.; Balakrishnan, M.; Subramanian, R. Synthesis, structural characterisation, optical studies of CeO_2 nanoparticles and its cytotoxic activity. *Mater. Res. Innov.* **2017**, *21*, 351–357. [CrossRef]
60. Hasanzadeh, L.; Oskuee, R.K.; Sadri, K.; Nourmohammadi, E.; Mohajeri, M.; Mardani, Z.; Hashemzadeh, A.; Darroudi, M. Green synthesis of labeled CeO_2 nanoparticles with 99mTc and its biodistribution evaluation in mice. *Life Sci.* **2018**, *212*, 233–240. [CrossRef]
61. Gupta, V.K.; Pal, R.; Siddiqi, N.J.; Sharma, B. Acetylcholinesterase from human erythrocytes as a surrogate biomarker of lead induced neurotoxicity. *Enzym. Res.* **2015**, *370705*, 1–7. [CrossRef]
62. Ali, M.S.; Ravikumar, S.; Beula, J.M. Bioactivity of seagrass against the dengue fever mosquito *Aedes aegypti* larvae. *Asian Pac. J. Trop. Biomed.* **2012**, *2*, 570–573. [CrossRef]
63. Dhavan, P.P.; Ranjana; Jadhav, B.L. Mosquito larvicidal potency of selected halophyte species and their modulation on acetylcholinesterase and glutathione s-transferase against dengue vector: *Aedes aegypti*. *Plant Cell Biotechnol. Mol. Biol.* **2022**, *23*, 1–14. [CrossRef]
64. Putri, G.E.; Rilda, Y.; Syukri, S.; Labanni, A.; Arief, S. Highly antimicrobial activity of cerium oxide nanoparticles synthesized using *Moringa oleifera* leaf extract by a rapid green precipitation method. *J. Mater. Res. Technol.* **2021**, *15*, 2355–2364. [CrossRef]
65. Sabouri, Z.; Sabouri, M.; Amiri, M.S.; Khatami, M.; Darroudi, M. Plant-based synthesis of cerium oxide nanoparticles using *Rheum turkestanicum* extract and evaluation of their cytotoxicity and photocatalytic properties. *Mater. Technol.* **2022**, *37*, 555–568. [CrossRef]
66. Rezvani, E.; Hatamie, A.; Berahman, M.; Simchi, M.; Angizi, S.; Rahmati, R.; Kennedy, J.; Simchi, A. Synthesis, first-principle simulation, and application of three-dimensional ceria nanoparticles/graphene nanocomposite for non-enzymatic hydrogen peroxide detection. *J. Electrochem. Soc.* **2019**, *166*, H3167. [CrossRef]
67. Awwad, A.M.; Salem, N.M. Green synthesis of silver nanoparticles by Mulberry Leaves Extract. *Nanosci. Nanotechnol.* **2012**, *2*, 125–128. [CrossRef]
68. Dutta, D.; Mukherjee, R.; Patra, M.; Banik, M.; Dasgupta, R.; Mukherjee, M.; Basu, T. Green synthesized cerium oxide nanoparticle: A prospective drug against oxidative harm. *Colloids Surf. B Biointerfaces* **2016**, *147*, 45–53. [CrossRef]
69. Ahn, E.Y.; Jin, H.; Park, Y. Assessing the antioxidant, cytotoxic, apoptotic and wound healing properties of silver nanoparticles green-synthesized by plant extracts. *Mater. Sci. Eng. C* **2019**, *101*, 204–216. [CrossRef]
70. Gopinath, K.; Karthika, V.; Sundaravadivelan, C.; Gowri, S.; Arumugam, A. Mycogenesis of cerium oxide nanoparticles using *Aspergillus niger* culture filtrate and their applications for antibacterial and larvicidal activities. *J. Nanostruct. Chem.* **2015**, *5*, 295–303. [CrossRef]
71. Sundaravadivelan, C.; Nalini Padmanabhan, M.; Sivaprasath, P.; Kishmu, L. Biosynthesized silver nanoparticles from *Pedilanthus tithymaloides* leaf extract with anti-developmental activity against larval instars of *Aedes aegypti* L. (Diptera; Culicidae). *Parasitol. Res.* **2013**, *112*, 303–311. [CrossRef]
72. Fournier, D. Mutations of acetylcholinesterase which confer insecticide resistance in insect populations. *Chem.-Biol. Interact.* **2005**, *157*, 257–261. [CrossRef]
73. Suganthy, N.; Pandian, S.K.; Devi, K.P. Cholinesterase inhibitory effects of *Rhizophora lamarckii*, *Avicennia officinalis*, *Sesuvium portulacastrum* and *Suaeda monica*: Mangroves inhabiting an Indian coastal area (Vellar Estuary). *J. Enzym. Inhib. Med. Chem.* **2009**, *24*, 702–707. [CrossRef]
74. Lu, F.C. *Basic Toxicology: Fundamentals, Target Organs, and Risk Assessment*; Taylor and Francis: Washington, DC, USA, 1996.
75. Trang, A.; Khandhar, P.B. Physiology, acetylcholinesterase. In *StatPearls [Internet]*; StatPearls Publishing: Treasure Island, FL, USA, 2021.
76. Vanhaelen, N.; Haubruge, E.; Lognay, G.; Francis, F. Hoverfly glutathione S-transferases and effect of Brassicaceae secondary metabolites. *Pestic. Biochem. Physiol.* **2001**, *71*, 170–177. [CrossRef]
77. Parkes, T.L.; Hilliker, A.J.; Phillips, J.P. Genetic and biochemical analysis of glutathione-S-transferase in the oxygen defense system of Drosophila melanogaster. *Genome* **1993**, *36*, 1007–1014. [CrossRef]
78. Giordano, G.; Afsharinejad, Z.; Guizzetti, M.; Vitalone, A.; Kavanagh, T.J.; Costa, L.G. Organophosphorus insecticides chlorpyrifos and diazinon and oxidative stress in neuronal cells in a genetic model of glutathione deficiency. *Toxicol. Appl. Pharmacol.* **2007**, *219*, 181–189. [CrossRef] [PubMed]
79. Vontas, J.G.; Small, G.J.; Hemingway, J. Glutathione S-transferases as antioxidant defence agents confer pyrethroid resistance in *Nilaparvata lugens*. *Biochem. J.* **2001**, *357*, 65–72. [CrossRef]
80. Dhavan, P.P.; Jadhav, B.L. Eco-friendly approach to control dengue vector *Aedes aegypti* larvae with their enzyme modulation by *Lumnitzera racemosa* fabricated zinc oxide nanorods. *SN Appl. Sci.* **2020**, *2*, 843. [CrossRef]

81. Vorbrodt, A. The role of phosphate in intracellular metabolism. *Postepy. Hig. Med. Dosw.* **1959**, *13*, 200–206.
82. Pratt, H.D. *Mosquitoes of Public Health Importance and Their Control (No. 772)*; US Department of Health, Education, and Welfare, Public Health Service, Communicable Disease Center: Atlanta, GA, USA, 1963.